

Smearing lattice gauge fields on a quantum computer

Erik Gustafson¹

¹*Fermi National Accelerator Laboratory, Batavia, Illinois 60510, USA*

(Dated: November 11, 2022)

Smearing of gauge-field configurations in lattice field theory improves the results of lattice simulations by suppressing high energy modes from correlation functions. In quantum simulations, high kinetic energy eigenstates are introduced when the time evolution operator is approximated such as Trotterization. While improved Trotter product formulae exist to reduce the errors, they have diminishing accuracy returns with respect to resource costs. Therefore having an algorithm that has fewer resources than an improved Trotter formula is desirable. In this work I develop a representation agnostic method for quantum smearing and show that it reduces the coupling to high energy modes in the discrete nonabelian gauge theory \mathbb{D}_4 .

1 Introduction. Classical lattice gauge theory (LGT) offers the ability for high precision determinations of observables such as decay constants, hadron masses, scattering amplitudes below multiparticle thresholds, finite temperature QCD, and equations of state [1–9]. However, these simulations struggle to extract multiparticle threshold final states and dynamical quantities such as viscosities which encounter sign problems using stochastic methods [10, 11]. Quantum computers offer a method to circumvent this sign problem entirely by using a Hamiltonian formulation for the deterministic evolution of a quantum system [12–14].

There has been a significant effort to develop methods for simulating LGTs on quantum computers [15–73]. The benefits for high energy physics from quantum simulators stems from the ability to do real-time simulations and study finite density physics. However it is known that many time evolution methods introduce couplings to other energy modes which is undesirable [40, 74, 75].

Implementations of the time evolution operator for quantum simulations involve approximating this operator [76–86]. One method, Trotterization, break the Hamiltonian, H , is broken into commuting terms, e.g. potential (V) and kinetic (K), such that $e^{itH} \approx (e^{i\delta t/2K} e^{-i\delta tV} e^{i\delta t/2K})^{t/\delta t}$, which are easily implemented on a quantum computer [76, 77, 87]. All approximations distort the Hamiltonian spectrum. Trotterization affects the spectrum by introducing terms proportional to $(t/n)^3$ multiplied by commutators such as $[K, [V, [V, K]]$; this significantly affects observables such as time dependent correlation functions [74]. The spectrum distortion induces couplings to other energy states [75, 88]. Therefore one wants a band-pass filter that cuts out the energy modes unconnected to the states of interest; higher order Trotter product formulae do this [77]. However, higher order Trotter products become increasingly more expensive in terms of gates and have diminishing accuracy returns [89]. The gate costs for quantum electrodynamics (QED) and quantum chromodynamics (QCD) simulations in Ref. [90] is expensive; therefore, finding methods to bring these costs down is crucial. One method would be finding an alternative way to bring down the systematic errors from approximate time evolution (APE) other than improved

operators.

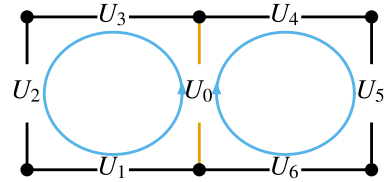


FIG. 1. Depiction of the plaquettes connected to a link in 2d. The orange line indicates the link to be smeared and the blue circles indicate the plaquettes that are taken as inputs to the smearing algorithm.

Classical LGT theory developed tools such as smearing [91–100] and gradient flow [101–104] as a method for dealing with high energy states in lattice configurations. This allows for classical simulations with $100 \times -1000 \times$ fewer statistics and coarser lattices [100, 105–107]. All smearing methods averages neighboring fluctuations on a lattice configuration to remove ultraviolet (UV) contamination; gradient flow moves the configuration along the renormalization group and dampens high-momentum field modes which can be used as a continuous method of smearing [102, 103, 108, 109]. In addition smearing comes in two forms: operator smearing and link smearing. Operator smearing mitigates the excited state contamination from a lattice operator choices, link smearing suppresses the noise from UV fluctuations from the background field configurations themselves. Since one does not know the UV state explicitly one approximates them by the using the kinetic energy operator as a proxy.

Therefore one would like to have a quantum equivalent of classical lattice link smearing that is both cost effective and removes some couplings to high energy modes induced by approximate time evolution or state preparation. The quantum case of smearing can be understood as introducing a small imaginary component to the kinetic energy operator that will suppress their contribution to time dependent observables. In many cases these non-unitary algorithms can yield shorter local circuits than their unitary counter parts at the expense of some probability of failure [40, 110–114].

In this context one can estimate the cost of smearing for a larger group that could approximate QCD, $S(1080)$.

Using the chosen smearing strength is $\rho = 0.2$ from Ref [115] as an approximate value for the smearing parameter used for a quantum simulation of $S(1080)$, the quantum smearing operator has an approximate nonunitarity of $\eta = 0.0005$ for a single link using the definition of η in Ref. [116]. If one estimates that a stochastic implementation such as in [113] of the non-unitary operator succeeds with probability $1 - \eta$, then every time all the links are smeared it will succeed with probability $(1 - \eta)^{d \cdot L^d}$ where d is the number of dimensions and L is the number of sites on the lattice in one direction. Using the volume as an estimate for gluon viscosity from Ref. [90], this would imply that for a 10^3 lattice using smearing 50 times would succeed stochastically with probability 10^{-33} . This is nearly impossible and the unitary method provided in this work would win out even with a subexponential increase in the number of required qubits.

In this letter, I develop a unitary quantum smearing algorithm based on classical stout smearing in a representation agnostic way. This quantum smearing algorithm scales linearly with the number of qubits and circuit depth compared to exponential costs with nonunitary operators. Using a discrete nonabelian gauge theory on a 2×1 lattice I demonstrate that the high energy modes are suppressed and the underlying physics is not distorted.

2 Stout smearing as a classical algorithm. Stout smearing takes a linear combination of plaquettes connected to a link, see Fig. 1, and then uses an exponential mapping of the linear combinations to transform the target link to a smeared link. The benefits of this smearing algorithm are that it smears out fluctuations at the lattice scale, preserves group structure, and is gauge invariant. Following the notation in Ref. [97], I cover the basics of stout smearing.

The staples connected to our target link $U_\mu(n)$ in the direction ν are defined as

$$C_{\mu,\nu}(n) = U_\nu(n)U_\mu(n + \hat{\nu})U_\nu^\dagger(n + \hat{\mu}) + U_\nu(n - \hat{\nu})^\dagger U_\mu(n - \hat{\nu})U_\nu(n - \hat{\nu} + \hat{\mu}); \quad (1)$$

this is the sum of the plaquettes in Fig. 1. Next, one defines the linear combination of plaquettes as

$$\Omega_\mu(U_\mu(n)) = \Omega_\mu(n) = \sum_{\nu \neq \mu} C_{\mu,\nu}(n)U_\mu^\dagger(n). \quad (2)$$

A new variable, $\mathcal{Q}_\mu(n)$, defined as

$$\mathcal{Q}_\mu(n) = \frac{i}{2} \left(\Omega_\mu(n) - \Omega_\mu^\dagger(n) - \frac{1}{N} \text{Tr}(\Omega_\mu(n) - \Omega_\mu^\dagger(n)) \right), \quad (3)$$

creates a traceless Hermitian matrix which is a generator for a group element. The target link is then transformed to

$$U'_\mu(n) = \mathcal{P}\{e^{-i\rho\mathcal{Q}_\mu(n)}\}U_\mu(n), \quad (4)$$

where ρ is a tunable parameter to determine how strong the smearing is and \mathcal{P} indicates that some projection back

onto the group may be required if the group is not sufficiently continuous. Hereinafter the element $\mathcal{P}\{e^{-i\rho\mathcal{Q}(n)}\}$ will be referred to as the shift element, $\mathcal{S}(\rho, \mathcal{Q})$. A graphical depiction of these terms is shown in Fig. 1.

3 Stout smearing as a quantum algorithm. A direct mapping of smearing encounters difficulties because it requires making a copy of the lattice; this is not allowed in quantum computation [117–121]. The copying procedure is required to avoid stroboscopic approximations. Therefore we need to alter the smearing algorithm to allow for reversibility which increases the required physical quantum resources compared to the classical algorithm.

Before introducing the algorithm, I will cover the necessary quantum operations needed for this algorithm. One requires three primitive group operations: \mathfrak{U}_\times which multiplies two group elements together, \mathfrak{U}_{-1} which inverts a group element, and $\mathcal{S}(\rho, \mathcal{Q})$ which generates the shift elements. The algorithm is summarized in Fig. 2.

```

for Link,  $U_\mu(n)$ , on the lattice do
  Store each plaquette in Eq. (2) onto scratch registers.
  Generate the link variable corresponding to  $\mathcal{S}(\rho, \mathcal{Q})$ .
  uncompute the plaquettes on the scratch register
end for
for Link,  $U_\mu(n)$ , on the lattice do
  Multiply the register with  $\mathcal{S}(\rho, \mathcal{Q})$  to respective  $U_\mu(n)$ .
end for

```

FIG. 2. Pseudocode describing the quantum stout smearing algorithm.

This algorithm is representation agnostic; any Hamiltonian formulation requires a method to represent group element basis states. However, the process of implementing \mathfrak{U}_\times , \mathfrak{U}_{-1} , and $\mathcal{S}(\rho, \mathcal{Q})$ is representation dependent. Nevertheless, given group element basis exists this the function $\mathcal{S}(\rho, \mathcal{Q})$ is equivalent to a function that takes as inputs numbers and outputs a new number onto a clean scratch register which is a valid unitary operation on a quantum computer [117]. A side effect of this algorithm is that a new lattice's worth of qubits is required every time the smearing operation is applied in order to ensure reversibility. Therefore there is a linear cost in the number of qubits to use this algorithm.

We show in Fig. 3 how to construct the state $|\mathcal{S}(\rho, \mathcal{Q})\rangle$ on an ancilla register for any group and formulation. It is straight forward once all shift elements have been constructed to multiply these elements with their corresponding physical lattice link using the \mathfrak{U}_\times operator.

4 \mathbb{D}_4 gauge theory example. It is illustrative to demonstrate smearing by a using discrete group which has the benefit of being defined explicitly in the group element basis. A dihedral group, \mathbb{D}_4 , whose primitive gates have been derived in Refs. [122, 123], is useful as a proof of principle example. The elements of the group are $g = (\sigma^x)^a (e^{i\pi/2\sigma^z})^{2b+c}$ with $0 \leq a, b, c \leq 1$ and σ^x and σ^z are two of the Pauli matrices. A group element $|g\rangle$ is represented by the qubit state $|abc\rangle$. This example uses a

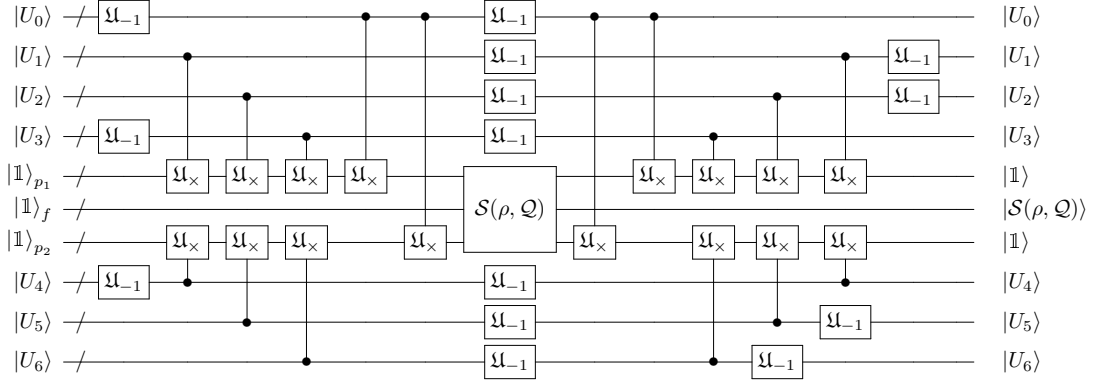


FIG. 3. Quantum circuit for constructing the projected element $\mathcal{S}(\rho, \mathcal{Q})$ on a 2d lattice. The forward slash indicates that the register maybe composed of multiple qubits. The registers $|U_m\rangle$ correspond to the links in Fig. 1. The three register gate $\mathcal{S}(\rho, \mathcal{Q})$ takes the $|\mathbb{1}\rangle_{p_1}$ and $|\mathbb{1}\rangle_{p_2}$ scratch plaquette registers as inputs and outputs the closest group element to $e^{i\rho\mathcal{Q}}$ onto the scratch register $|\mathbb{1}\rangle_f$.

two plaquette theory with periodic boundary conditions as shown in Fig. 4 The Hamiltonian for this theory is

$$H = -\beta(\text{ReTr}(U_0 U_1 U_2^\dagger U_1^\dagger + U_2 U_3 U_0^\dagger U_3^\dagger)) + \log(T_K), \quad (5)$$

where $\log(T_K)$ is the kinetic term of the Hamiltonian, K , and is defined in [122] and $-\beta(\text{ReTr}(U_0 U_1 U_2^\dagger U_1^\dagger + U_2 U_3 U_0^\dagger U_3^\dagger))$ is the potential term of the Hamiltonian, V . In this example $\beta = 0.75$.

An implementation of $\mathcal{S}(\rho, \mathcal{Q})$ for \mathbb{D}_4 is necessary. The realization of the circuit depends on the chosen value of ρ . In order to ensure that smearing occurs but is not too significant that it distorts the underlying physics, let $\rho = 0.26$. For ρ less than this value no smearing will take place. Since \mathbb{D}_4 is discrete, ρ within given ranges will yield the same $\mathcal{S}(\rho, \mathcal{Q})$. Fig. 5 shows the implementation of this quantum circuit for $\rho = 0.26$. The time evolution operator $\mathbf{U}_n(t) = e^{-itH}$, where n is the Trotterization order, is at second order

$$\mathbf{U}_2(t; \delta t) = (e^{-i\delta t/2K} e^{-i\delta t V} e^{-i\delta t/2K})^{t/\delta t}, \quad (6)$$

and third order

$$\mathbf{U}_3(t; \delta t) = (e^{-i7\delta t V/24} e^{-i2\delta t K/3} e^{-i3\delta t V/4} e^{i2\delta t K/3} e^{-i\delta t V/24} e^{-i\delta t K})^{t/\delta t} \quad (7)$$

where K and V are the kinetic and potential parts of the Hamiltonian. For these simulations $\delta t = 0.85$. This is an example which shows contributions from other eigenstates.

Fig. 6 shows the time evolution with $\delta t = 0.85$, of the plaquette correlator,

$$\langle P(t) \rangle = \langle \Omega | U^\dagger(t; \delta t) P U(t; \delta t) | F \rangle, \quad (8)$$

where $\langle \Omega |$ is the gauge invariant ground state, $|F\rangle$ is the gauge invariant projection of the first excited state, and P is the plaquette $\text{ReTr}(U_0 U_1 U_2^\dagger U_1^\dagger)$. A third order

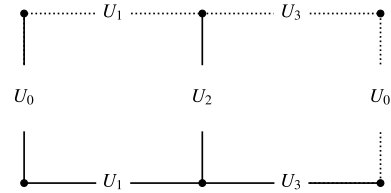


FIG. 4. 2 Plaquette lattice for the \mathbb{D}_4 simulation. The dashed lines indicate repeated links from periodic boundary conditions.

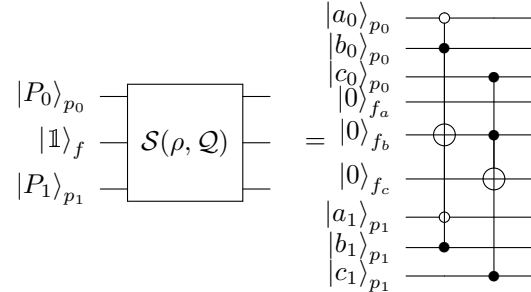


FIG. 5. Quantum Circuit that implements the operator $\mathcal{S}(\rho = 0.26, \mathcal{Q})$ for \mathbb{D}_4 .

Trotterization at $\delta t = 1.0$ which has nearly the same root mean square error as the smeared evolution is also shown. While the third order Trotterization is superior to the second order Trotterization with and with out smearing before $t = 10$, afterwards the higher energy states begin to distort the time evolution which is expected for a coarse Trotterization and aligns with the second order smeared Trotterization. The ancilla registers are reset in order to minimize the memory resource requirements on the classical simulations.

It is worth examining the resource costs of smearing in a fault tolerant perspective. Many error correcting codes for fault tolerant quantum computing have costly single qubit rotation operations such as the T-gate [124–

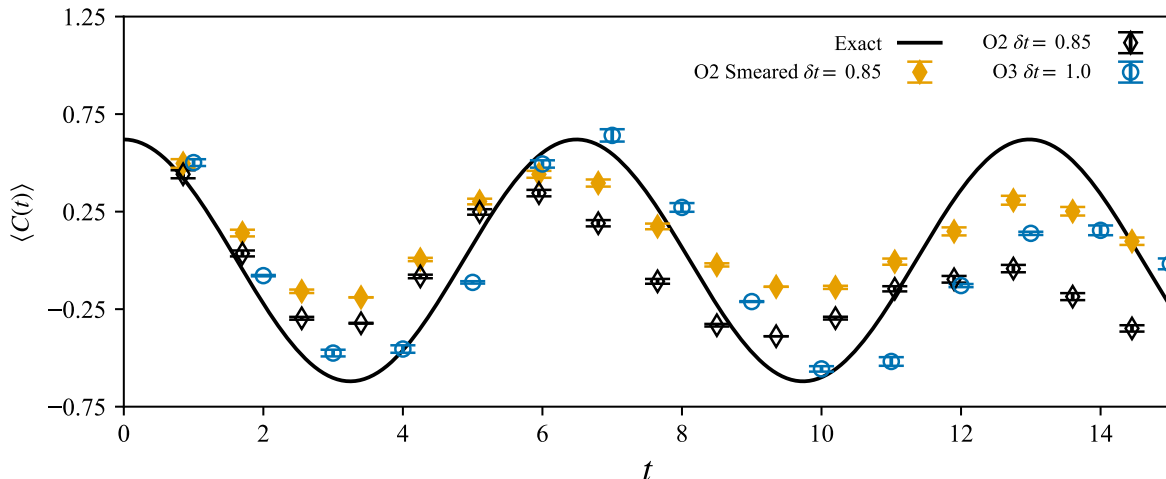


FIG. 6. Time evolution of the correlators $C(t)$, at $\beta = 0.85$ for second order Trotterization, O2, with and without smearing and third order Trotterization, O3, at $\delta t = 1.2$ for equivalent accuracy.

129]. For this reason T-gates are an important metric for algorithm costs on fault tolerant quantum computers.

TABLE I. T gate costs for various operations per Trotter step for the whole system on a 2×1 plaquette lattice for \mathbb{D}_4 .

operator	T gates
2^{nd} order Trotter	$696 + 46\log_2(1/\epsilon)$
3^{rd} order Trotter	$1008 + 131.1\log_2(1/\epsilon)$
smearing	560

The T-gate costs of a single second order Trotter step for \mathbb{D}_4 , third order Trotter, and the smearing operator on the whole lattice in Tab. I. These costs are derived from the gates provided in Refs. [122, 123] and the single qubit gates are approximated using the repeat until success method with T gate cost $1.15\log_2(1/\epsilon)$ where ϵ is the desired gate infidelity [130]. The total cost for third order Trotterization for infidelity, $\epsilon = 10^{-8}$ and $\delta t = 1$ requires 1.75 times more T gates than a second order Trotterization at $\delta t = 0.85$ with smearing and 2.5 times as many T-gates if the third order Trotterization is used with $\delta t = 0.85$. This T gate saving should increase for larger groups as the projection operation will not require approximations using T-gate synthesis. The second order smeared evolution has fewer high energy oscillations than the unsmeared evolution. Information regarding energy states can be extracted from the fourier spectrum of the time series data. Examining the Fourier spectrum for the smeared and unsmeared evolution using second order Trotterization (see Fig. 7) shows that many high kinetic energy modes are mitigated. It is found that smearing does not uniformly suppress higher order energies.

5. *Conclusions* This work developed a unitary algorithm for smearing real-time quantum simulations of LGTs. Somewhat analogously to classical LGT, this algorithm acts as expected by reducing higher energy modes. For the small lattice size investigated the benefits of smearing are noticable and achieves a factor of 2 reduction

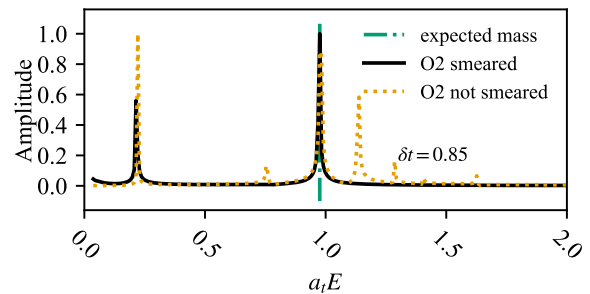


FIG. 7. Comparison of the energy spectrum with and without smearing at $\delta t = 0.85$ using second order Trotterization denoted O2.

in T-gates compared to improved Trotterization. The computational costs scale linearly with the number of times smearing is applied compared to exponential costs for nonunitary evolution. The representation agnostic method in which this algorithm is presented allows it to be applied to a wide range of Hamiltonian formulations [43, 50, 71, 115, 123, 131–149] for quantum simulation of LGTs and will likely bring down the cost of many fault tolerant applications. This opens the way to build smearing algorithms for larger groups that could approximate $SU(3)$ and $SU(2)$ as well as extend the method to the inclusion of dynamical fermions.

ACKNOWLEDGMENTS

I wish to thank Mike Wagman, Ruth Van de Water, Norman Tubman, Stuart Hadfield, Henry Lamm, Judah Unmuth-Yockey, and Matthew Reagor for comments and advice. This work is supported by the DOE QuantISED program through the theory consortium “Intersections of QIS and Theoretical Particle Physics” at Fermilab and by the U.S. Department of Energy. Fermilab is operated by Fermi Research Alliance, LLC under contract number DE-AC02-07CH11359 with the United States Department

-
- [1] W. Detmold, R. G. Edwards, J. J. Dudek, M. Engelhardt, H.-W. Lin, S. Meinel, K. Orginos, and P. Shanahan (USQCD), Hadrons and Nuclei, *Eur. Phys. J. A* **55**, 193 (2019), [arXiv:1904.09512 \[hep-lat\]](#).
- [2] T. Aoyama *et al.*, The anomalous magnetic moment of the muon in the Standard Model, *Phys. Rept.* **887**, 1 (2020), [arXiv:2006.04822 \[hep-ph\]](#).
- [3] Y. Aoki *et al.* (Flavour Lattice Averaging Group (FLAG)), FLAG Review 2021, *Eur. Phys. J. C* **82**, 869 (2022), [arXiv:2111.09849 \[hep-lat\]](#).
- [4] A. S. Kronfeld *et al.* (USQCD), Lattice QCD and Particle Physics (2022), [arXiv:2207.07641 \[hep-lat\]](#).
- [5] A. Bazavov, F. Karsch, S. Mukherjee, and P. Petreczky (USQCD), Hot-dense Lattice QCD: USQCD whitepaper 2018, *Eur. Phys. J. A* **55**, 194 (2019), [arXiv:1904.09951 \[hep-lat\]](#).
- [6] P. A. Boyle *et al.*, A lattice QCD perspective on weak decays of b and c quarks Snowmass 2022 White Paper, in *2022 Snowmass Summer Study* (2022) [arXiv:2205.15373 \[hep-lat\]](#).
- [7] A. S. Kronfeld, D. G. Richards, W. Detmold, R. Gupta, H.-W. Lin, K.-F. Liu, A. S. Meyer, R. Sufian, and S. Syritsyn (USQCD), Lattice QCD and Neutrino-Nucleus Scattering, *Eur. Phys. J. A* **55**, 196 (2019), [arXiv:1904.09931 \[hep-lat\]](#).
- [8] Z. Davoudi *et al.*, Report of the Snowmass 2021 Topical Group on Lattice Gauge Theory, in *2022 Snowmass Summer Study* (2022) [arXiv:2209.10758 \[hep-lat\]](#).
- [9] R. A. Briceño, J. J. Dudek, and R. D. Young, Scattering processes and resonances from lattice QCD, *Reviews of Modern Physics* **90**, 10.1103/revmodphys.90.025001 (2018).
- [10] P. de Forcrand, Simulating QCD at finite density, *PoS LAT2009*, 010 (2009), [arXiv:1005.0539 \[hep-lat\]](#).
- [11] R.-A. Tripolt, P. Gubler, M. Ulybyshev, and L. Von Smekal, Numerical analytic continuation of Euclidean data, *Comput. Phys. Commun.* **237**, 129 (2019), [arXiv:1801.10348 \[hep-ph\]](#).
- [12] R. P. Feynman, Simulating physics with computers, *Int. J. Theor. Phys.* **21**, 467 (1982).
- [13] S. P. Jordan, K. S. M. Lee, and J. Preskill, Quantum Computation of Scattering in Scalar Quantum Field Theories, *Quant. Inf. Comput.* **14**, 1014 (2014), [arXiv:1112.4833 \[hep-th\]](#).
- [14] S. P. Jordan, K. S. M. Lee, and J. Preskill, Quantum Algorithms for Quantum Field Theories, *Science* **336**, 1130 (2012), [arXiv:1111.3633 \[quant-ph\]](#).
- [15] D. Banerjee, M. Dalmonte, M. Muller, E. Rico, P. Stebler, U. J. Wiese, and P. Zoller, Atomic Quantum Simulation of Dynamical Gauge Fields coupled to Fermionic Matter: From String Breaking to Evolution after a Quench, *Phys. Rev. Lett.* **109**, 175302 (2012), [arXiv:1205.6366 \[cond-mat.quant-gas\]](#).
- [16] N. Mueller, J. A. Carolan, A. Connelly, Z. Davoudi, E. F. Dumitrescu, and K. Yeter-Aydeniz, Quantum computation of dynamical quantum phase transitions and entanglement tomography in a lattice gauge theory (2022), [arXiv:2210.03089 \[quant-ph\]](#).
- [17] A. Ciavarella, N. Klco, and M. J. Savage, Some Conceptual Aspects of Operator Design for Quantum Simulations of Non-Abelian Lattice Gauge Theories (2022) [arXiv:2203.11988 \[quant-ph\]](#).
- [18] E. Zohar, J. I. Cirac, and B. Reznik, Simulating Compact Quantum Electrodynamics with ultracold atoms: Probing confinement and nonperturbative effects, *Phys. Rev. Lett.* **109**, 125302 (2012), [arXiv:1204.6574 \[quant-ph\]](#).
- [19] E. Zohar, J. I. Cirac, and B. Reznik, Cold-Atom Quantum Simulator for SU(2) Yang-Mills Lattice Gauge Theory, *Phys. Rev. Lett.* **110**, 125304 (2013), [arXiv:1211.2241 \[quant-ph\]](#).
- [20] E. Zohar, J. I. Cirac, and B. Reznik, Quantum simulations of gauge theories with ultracold atoms: local gauge invariance from angular momentum conservation, *Phys. Rev. A* **88**, 023617 (2013), [arXiv:1303.5040 \[quant-ph\]](#).
- [21] E. Zohar and M. Burrello, Formulation of lattice gauge theories for quantum simulations, *Phys. Rev. D* **91**, 054506 (2015), [arXiv:1409.3085 \[quant-ph\]](#).
- [22] E. Zohar, J. I. Cirac, and B. Reznik, Quantum Simulations of Lattice Gauge Theories using Ultracold Atoms in Optical Lattices, *Rept. Prog. Phys.* **79**, 014401 (2016), [arXiv:1503.02312 \[quant-ph\]](#).
- [23] E. Zohar, A. Farace, B. Reznik, and J. I. Cirac, Digital lattice gauge theories, *Phys. Rev. A* **95**, 023604 (2017), [arXiv:1607.08121 \[quant-ph\]](#).
- [24] N. Klco, J. R. Stryker, and M. J. Savage, SU(2) non-Abelian gauge field theory in one dimension on digital quantum computers, *Phys. Rev. D* **101**, 074512 (2020), [arXiv:1908.06935 \[quant-ph\]](#).
- [25] A. Ciavarella, N. Klco, and M. J. Savage, A Trailhead for Quantum Simulation of SU(3) Yang-Mills Lattice Gauge Theory in the Local Multiplet Basis (2021), [arXiv:2101.10227 \[quant-ph\]](#).
- [26] J. Bender, E. Zohar, A. Farace, and J. I. Cirac, Digital quantum simulation of lattice gauge theories in three spatial dimensions, *New J. Phys.* **20**, 093001 (2018), [arXiv:1804.02082 \[quant-ph\]](#).
- [27] J. Liu and Y. Xin, Quantum simulation of quantum field theories as quantum chemistry (2020), [arXiv:2004.13234 \[hep-th\]](#).
- [28] D. C. Hackett, K. Howe, C. Hughes, W. Jay, E. T. Neil, and J. N. Simone, Digitizing Gauge Fields: Lattice Monte Carlo Results for Future Quantum Computers, *Phys. Rev. A* **99**, 062341 (2019), [arXiv:1811.03629 \[quant-ph\]](#).
- [29] A. Alexandru, P. F. Bedaque, S. Harmalkar, H. Lamm, S. Lawrence, and N. C. Warrington (NuQS), Gluon field digitization for quantum computers, *Phys. Rev. D* **100**, 114501 (2019), [arXiv:1906.11213 \[hep-lat\]](#).
- [30] A. Yamamoto, Real-time simulation of (2+1)-dimensional lattice gauge theory on qubits, *PTEP* **2021**, 013B06 (2021), [arXiv:2008.11395 \[hep-lat\]](#).
- [31] J. F. Haase, L. Dellantonio, A. Celi, D. Paulson, A. Kan, K. Jansen, and C. A. Muschik, A resource efficient approach for quantum and classical simulations of gauge theories in particle physics, *Quantum* **5**, 393 (2021), [arXiv:2006.14160 \[quant-ph\]](#).

- [32] T. Armon, S. Ashkenazi, G. García-Moreno, A. González-Tudela, and E. Zohar, Photon-mediated Stroboscopic Quantum Simulation of a Z_2 Lattice Gauge Theory (2021), [arXiv:2107.13024 \[quant-ph\]](#).
- [33] A. Bazavov, S. Catterall, R. G. Jha, and J. Unmuth-Yockey, Tensor renormalization group study of the non-abelian higgs model in two dimensions, *Phys. Rev. D* **99**, 114507 (2019).
- [34] M. Honda, E. Itou, Y. Kikuchi, and Y. Tanizaki, Negative string tension of a higher-charge Schwinger model via digital quantum simulation, *PTEP* **2022**, 033B01 (2022), [arXiv:2110.14105 \[hep-th\]](#).
- [35] A. Bazavov, Y. Meurice, S.-W. Tsai, J. Unmuth-Yockey, and J. Zhang, Gauge-invariant implementation of the Abelian Higgs model on optical lattices, *Phys. Rev.* **D92**, 076003 (2015), [arXiv:1503.08354 \[hep-lat\]](#).
- [36] J. Zhang, J. Unmuth-Yockey, J. Zeiher, A. Bazavov, S. W. Tsai, and Y. Meurice, Quantum simulation of the universal features of the Polyakov loop, *Phys. Rev. Lett.* **121**, 223201 (2018), [arXiv:1803.11166 \[hep-lat\]](#).
- [37] J. Unmuth-Yockey, J. Zhang, A. Bazavov, Y. Meurice, and S.-W. Tsai, Universal features of the Abelian Polyakov loop in 1+1 dimensions, *Phys. Rev.* **D98**, 094511 (2018), [arXiv:1807.09186 \[hep-lat\]](#).
- [38] J. F. Unmuth-Yockey, Gauge-invariant rotor Hamiltonian from dual variables of 3D $U(1)$ gauge theory, *Phys. Rev. D* **99**, 074502 (2019), [arXiv:1811.05884 \[hep-lat\]](#).
- [39] M. Kreshchuk, W. M. Kirby, G. Goldstein, H. Beauchemin, and P. J. Love, Quantum Simulation of Quantum Field Theory in the Light-Front Formulation (2020), [arXiv:2002.04016 \[quant-ph\]](#).
- [40] E. Gustafson, Projective Cooling for the transverse Ising model, *Phys. Rev. D* **101**, 071504 (2020), [arXiv:2002.06222 \[hep-lat\]](#).
- [41] E. Gustafson, B. Holzman, J. Kowalkowski, H. Lamm, A. C. Y. Li, G. Perdue, S. Boixo, S. Isakov, O. Martin, R. Thomson, C. Vollgraaf Heidweiller, J. Beall, M. Ganahl, G. Vidal, and E. Peters, Large scale multi-node simulations of Z_2 gauge theory quantum circuits using Google Cloud Platform, [arXiv e-prints](#), [arXiv:2110.07482](#) (2021), [arXiv:2110.07482 \[quant-ph\]](#).
- [42] M. Kreshchuk, S. Jia, W. M. Kirby, G. Goldstein, J. P. Vary, and P. J. Love, Simulating Hadronic Physics on NISQ devices using Basis Light-Front Quantization (2020), [arXiv:2011.13443 \[quant-ph\]](#).
- [43] I. Raychowdhury and J. R. Stryker, Solving Gauss's Law on Digital Quantum Computers with Loop-String-Hadron Digitization (2018), [arXiv:1812.07554 \[hep-lat\]](#).
- [44] I. Raychowdhury and J. R. Stryker, Loop, String, and Hadron Dynamics in $SU(2)$ Hamiltonian Lattice Gauge Theories, *Phys. Rev. D* **101**, 114502 (2020), [arXiv:1912.06133 \[hep-lat\]](#).
- [45] B. Chakraborty, M. Honda, T. Izubuchi, Y. Kikuchi, and A. Tomiya, Classically emulated digital quantum simulation of the Schwinger model with a topological term via adiabatic state preparation, *Phys. Rev. D* **105**, 094503 (2022), [arXiv:2001.00485 \[hep-lat\]](#).
- [46] H.-Y. Wang, W.-Y. Zhang, Z.-Y. Yao, Y. Liu, Z.-H. Zhu, Y.-G. Zheng, X.-K. Wang, H. Zhai, Z.-S. Yuan, and J.-W. Pan, Interrelated Thermalization and Quantum Criticality in a Lattice Gauge Simulator (2022), [arXiv:2210.17032 \[cond-mat.quant-gas\]](#).
- [47] Z. Davoudi, I. Raychowdhury, and A. Shaw, Search for efficient formulations for Hamiltonian simulation of non-Abelian lattice gauge theories, *Phys. Rev. D* **104**, 074505 (2021), [arXiv:2009.11802 \[hep-lat\]](#).
- [48] U.-J. Wiese, Towards Quantum Simulating QCD, *Proceedings, 24th International Conference on Ultra-Relativistic Nucleus-Nucleus Collisions (Quark Matter 2014): Darmstadt, Germany, May 19-24, 2014*, *Nucl. Phys.* **A931**, 246 (2014), [arXiv:1409.7414 \[hep-th\]](#).
- [49] D. Luo, J. Shen, M. Highman, B. K. Clark, B. DeMarco, A. X. El-Khadra, and B. Gadway, A Framework for Simulating Gauge Theories with Dipolar Spin Systems (2019), [arXiv:1912.11488 \[quant-ph\]](#).
- [50] R. C. Brower, D. Berenstein, and H. Kawai, Lattice Gauge Theory for a Quantum Computer, *PoS LATTICE2019*, 112 (2020), [arXiv:2002.10028 \[hep-lat\]](#).
- [51] S. V. Mathis, G. Mazzola, and I. Tavernelli, Toward scalable simulations of Lattice Gauge Theories on quantum computers, *Phys. Rev. D* **102**, 094501 (2020), [arXiv:2005.10271 \[quant-ph\]](#).
- [52] H. Singh, Qubit $O(N)$ nonlinear sigma models (2019), [arXiv:1911.12353 \[hep-lat\]](#).
- [53] H. Singh and S. Chandrasekharan, Qubit regularization of the $O(3)$ sigma model, *Phys. Rev. D* **100**, 054505 (2019), [arXiv:1905.13204 \[hep-lat\]](#).
- [54] A. J. Buser, T. Bhattacharya, L. Cincio, and R. Gupta, Quantum simulation of the qubit-regularized $O(3)$ -sigma model (2020), [arXiv:2006.15746 \[quant-ph\]](#).
- [55] T. Bhattacharya, A. J. Buser, S. Chandrasekharan, R. Gupta, and H. Singh, Qubit regularization of asymptotic freedom (2020), [arXiv:2012.02153 \[hep-lat\]](#).
- [56] J. a. Barata, N. Mueller, A. Tarasov, and R. Venugopalan, Single-particle digitization strategy for quantum computation of a ϕ^4 scalar field theory (2020), [arXiv:2012.00020 \[hep-th\]](#).
- [57] M. Kreshchuk, S. Jia, W. M. Kirby, G. Goldstein, J. P. Vary, and P. J. Love, Light-Front Field Theory on Current Quantum Computers (2020), [arXiv:2009.07885 \[quant-ph\]](#).
- [58] Y. Ji, H. Lamm, and S. Zhu (NuQS), Gluon Field Digitization via Group Space Decimation for Quantum Computers, *Phys. Rev. D* **102**, 114513 (2020), [arXiv:2005.14221 \[hep-lat\]](#).
- [59] C. W. Bauer and D. M. Grabowska, Efficient Representation for Simulating $U(1)$ Gauge Theories on Digital Quantum Computers at All Values of the Coupling (2021), [arXiv:2111.08015 \[hep-ph\]](#).
- [60] E. Gustafson, Prospects for Simulating a Qudit Based Model of (1+1)d Scalar QED, *Phys. Rev. D* **103**, 114505 (2021), [arXiv:2104.10136 \[quant-ph\]](#).
- [61] T. Hartung, T. Jakobs, K. Jansen, J. Ostmeyer, and C. Urbach, Digitising $SU(2)$ gauge fields and the freezing transition, *Eur. Phys. J. C* **82**, 237 (2022), [arXiv:2201.09625 \[hep-lat\]](#).
- [62] D. M. Grabowska, C. Kane, B. Nachman, and C. W. Bauer, Overcoming exponential scaling with system size in Trotter-Suzuki implementations of constrained Hamiltonians: 2+1 $U(1)$ lattice gauge theories (2022), [arXiv:2208.03333 \[quant-ph\]](#).
- [63] E. M. Murairi, M. J. Cervia, H. Kumar, P. F. Bedaque, and A. Alexandru, How many quantum gates do gauge theories require? (2022), [arXiv:2208.11789 \[hep-lat\]](#).
- [64] A. Jahin, A. C. Y. Li, T. Iadecola, P. P. Orth, G. N. Perdue, A. Macridin, M. Sohaib Alam, and N. M. Tubman, Fermionic approach to variational quantum simulation of Kitaev spin models, *Phys. Rev. A* **106**, 022434 (2022),

- arXiv:2204.05322 [quant-ph].
- [65] R. C. Farrell, I. A. Chernyshev, S. J. M. Powell, N. A. Zemlevskiy, M. Illa, and M. J. Savage, Preparations for Quantum Simulations of Quantum Chromodynamics in 1+1 Dimensions: (II) Single-Baryon β -Decay in Real Time (2022), arXiv:2209.10781 [quant-ph].
- [66] A. C. Y. Li, A. Macridin, S. Mrenna, and P. Spentzouris, Simulating scalar field theories on quantum computers with limited resources (2022), arXiv:2210.07985 [quant-ph].
- [67] R. C. Farrell, I. A. Chernyshev, S. J. M. Powell, N. A. Zemlevskiy, M. Illa, and M. J. Savage, Preparations for Quantum Simulations of Quantum Chromodynamics in 1+1 Dimensions: (I) Axial Gauge (2022), arXiv:2207.01731 [quant-ph].
- [68] R. Maxton and Y. Meurice, Perturbative boundaries of quantum computing: real-time evolution for digitized lambda phi^4 lattice models (2022), arXiv:2210.05493 [quant-ph].
- [69] M. Asaduzzaman, S. Catterall, G. C. Toga, Y. Meurice, and R. Sakai, Quantum Simulation of the N flavor Gross-Neveu Model (2022), arXiv:2208.05906 [hep-lat].
- [70] E. Gustafson, Noise Improvements in Quantum Simulations of sQED using Qutrits, arXiv e-prints , arXiv:2201.04546 (2022), arXiv:2201.04546 [quant-ph].
- [71] E. J. Gustafson, H. Lamm, F. Lovelace, and D. Musk, Primitive Quantum Gates for an SU(2) Discrete Subgroup: BT, arXiv e-prints , arXiv:2208.12309 (2022), arXiv:2208.12309 [quant-ph].
- [72] A. Janni, H. Lamm, and R. Van de Water, [Gluon Representation for Lattice QCD Computer Simulations](#).
- [73] A. N. Ciavarella and I. A. Chernyshev, Preparation of the SU(3) lattice Yang-Mills vacuum with variational quantum methods, *Phys. Rev. D* **105**, 074504 (2022), arXiv:2112.09083 [quant-ph].
- [74] M. Carena, H. Lamm, Y.-Y. Li, and W. Liu, Lattice Renormalization of Quantum Simulations, arXiv e-prints , arXiv:2107.01166 (2021), arXiv:2107.01166 [hep-lat].
- [75] A. M. Childs, Y. Su, M. C. Tran, N. Wiebe, and S. Zhu, A Theory of Trotter Error, arXiv e-prints , arXiv:1912.08854 (2019), arXiv:1912.08854 [quant-ph].
- [76] S. Lloyd, Universal quantum simulators, *Science* **273**, 1073 (1996).
- [77] M. Suzuki, Decomposition formulas of exponential operators and lie exponentials with some applications to quantum mechanics and statistical physics, *Journal of Mathematical Physics* **26**, 10.1063/1.526596 (1985), <https://doi.org/10.1063/1.526596>.
- [78] B. Commeau, M. Cerezo, Z. Holmes, L. Cincio, P. J. Coles, and A. Sornborger, Variational hamiltonian diagonalization for dynamical quantum simulation, arXiv preprint arXiv:2009.02559 (2020).
- [79] K. Bharti and T. Haug, Quantum Assisted Simulator, *Phys. Rev. A* **104**, 042418 (2021), arXiv:2011.06911 [quant-ph].
- [80] Y. Li and S. C. Benjamin, Efficient variational quantum simulator incorporating active error minimization, *Phys. Rev. X* **7**, 021050 (2017).
- [81] K. H. Lim, T. Haug, L. C. Kwek, and K. Bharti, Fast-Forwarding with NISQ Processors without Feedback Loop, *Quantum Sci. Technol.* **7**, 015001 (2021), arXiv:2104.01931 [quant-ph].
- [82] J. W. Z. Lau, T. Haug, L. C. Kwek, and K. Bharti, Nisq algorithm for hamiltonian simulation via truncated taylor series, *SciPost Physics* **12**, 122 (2022).
- [83] C. Zoufal, D. Sutter, and S. Woerner, Error bounds for variational quantum time evolution, arXiv preprint arXiv:2108.00022 (2021).
- [84] N. Zagury, A. Aragao, J. Casanova, and E. Solano, Unitary expansion of the time evolution operator, *Physical Review A* **82**, 042110 (2010).
- [85] S. Barison, F. Vicentini, and G. Carleo, An efficient quantum algorithm for the time evolution of parameterized circuits, *Quantum* **5**, 512 (2021).
- [86] X. Yuan, S. Endo, Q. Zhao, Y. Li, and S. C. Benjamin, Theory of variational quantum simulation, *Quantum* **3**, 191 (2019).
- [87] F. Casas and A. Murua, An efficient algorithm for computing the baker–campbell–hausdorff series and some of its applications, *Journal of Mathematical Physics* **50**, 033513 (2009), <https://doi.org/10.1063/1.3078418>.
- [88] A. M. Childs, D. Maslov, Y. Nam, N. J. Ross, and Y. Su, Toward the first quantum simulation with quantum speedup, *Proceedings of the National Academy of Science* **115**, 9456 (2018), arXiv:1711.10980 [quant-ph].
- [89] N. Wiebe, D. Berry, P. Høyer, and B. C. Sanders, Higher order decompositions of ordered operator exponentials, *Journal of Physics A Mathematical General* **43**, 065203 (2010), arXiv:0812.0562 [math-ph].
- [90] A. Kan and Y. Nam, Lattice quantum chromodynamics and electrodynamics on a universal quantum computer (2021), arXiv:2107.12769 [quant-ph].
- [91] W. Kamleh, D. H. Adams, D. B. Leinweber, and A. G. Williams, Accelerated overlap fermions, *Phys. Rev. D* **66**, 014501 (2002).
- [92] B. Joó, J. Karpie, K. Orginos, A. V. Radyushkin, D. G. Richards, R. S. Sufian, and S. Zafeiropoulos, Pion valence structure from ioffe-time parton pseudodistribution functions, *Physical Review D* **100**, 114512 (2019).
- [93] S. Güsken, R. Sommer, K.-H. Mütter, U. Löw, K. Schilling, and A. Patel, Non-singlet axial vector couplings of the baryon octet in lattice qcd, *Phys. Lett. B* **227**, 266 (1989).
- [94] C. Morningstar and M. Peardon, Analytic smearing of SU(3) link variables in lattice qcd, *Phys. Rev. D* **69**, 054501 (2004).
- [95] J. B. Zhang, P. J. Moran, P. O. Bowman, D. B. Leinweber, and A. G. Williams, Stout-link smearing in lattice fermion actions, *Phys. Rev. D* **80**, 074503 (2009), arXiv:0908.3726 [hep-lat].
- [96] F. Bruckmann, F. Gruber, C. B. Lang, M. Limmer, T. Maurer, A. Schäfer, and S. Solbrig, Comparison of filtering methods in SU(3) lattice gauge theory, arXiv e-prints , arXiv:0901.2286 (2009), arXiv:0901.2286 [hep-lat].
- [97] P. J. Moran and D. B. Leinweber, Over-improved stout-link smearing, *Phys. Rev. D* **77**, 094501 (2008), arXiv:0801.1165 [hep-lat].
- [98] S. Basak, I. Sato, S. Wallace, R. Edwards, D. Richards, G. T. Fleming, U. M. Heller, A. C. Lichtl, and C. Morningstar, Combining quark and link smearing to improve extended baryon operators, *PoS LAT2005*, 076 (2006), arXiv:hep-lat/0509179.
- [99] S. Güsken, A study of smearing techniques for hadron correlation functions, *Nuclear Physics B - Proceedings Supplements* **17**, 361 (1990).
- [100] M. Albanese, F. Costantini, G. Fiorentini, F. Flore, M. Lombardo, R. Tripiccone, P. Bacilieri, L. Fonti, P. Gi-

- acomelli, E. Remiddi, M. Bernaschi, N. Cabibbo, E. Marinari, G. Parisi, G. Salina, S. Cabasino, F. Marzano, P. Paolucci, S. Petrarca, F. Rapuano, P. Marchesini, and R. Rusack, Glueball masses and string tension in lattice qcd, *Physics Letters B* **192**, 163 (1987).
- [101] M. Luscher, Trivializing maps, the Wilson flow and the HMC algorithm, *Commun. Math. Phys.* **293**, 899 (2010), [arXiv:0907.5491 \[hep-lat\]](#).
- [102] M. Luscher and P. Weisz, Perturbative analysis of the gradient flow in non-abelian gauge theories, *JHEP* **02**, 051, [arXiv:1101.0963 \[hep-th\]](#).
- [103] C. Bonati and M. D'Elia, Comparison of the gradient flow with cooling in SU(3) pure gauge theory, *Phys. Rev. D* **89**, 105005 (2014), [arXiv:1401.2441 \[hep-lat\]](#).
- [104] M. Lüscher and P. Weisz, Perturbative analysis of the gradient flow in non-abelian gauge theories, *Journal of High Energy Physics* **2011**, 51 (2011), [arXiv:1101.0963 \[hep-th\]](#).
- [105] A. Hasenfratz and F. Knechtli, Flavor symmetry and the static potential with hypercubic blocking, *Phys. Rev. D* **64**, 034504 (2001), [arXiv:hep-lat/0103029 \[hep-lat\]](#).
- [106] S. Durr, Gauge action improvement and smearing, *Comput. Phys. Commun.* **172**, 163 (2005), [arXiv:hep-lat/0409141](#).
- [107] N. Karthik, *Studies on gauge-link smearing and their applications to lattice QCD at finite temperature*, Ph.D. thesis (2014).
- [108] D. Negradi, Z. Fodor, K. Holland, J. Kuti, S. Mondal, and C. H. Wong, The lattice gradient flow at tree level, *PoS LATTICE2014*, 328 (2014), [arXiv:1410.8801 \[hep-lat\]](#).
- [109] Z. Fodor, K. Holland, J. Kuti, D. Negradi, and C. H. Wong, The Yang-Mills gradient flow in finite volume, *JHEP* **11**, 007, [arXiv:1208.1051 \[hep-lat\]](#).
- [110] M. Hite, J. Hubisz, B. Sambasivam, J. Unmuth-Yockey, and E. Gustafson, Quantum Simulation of Open Lattice Field Theories, in *APS March Meeting Abstracts*, APS Meeting Abstracts, Vol. 2022 (2022) p. Q40.002.
- [111] D. Lee, J. Bonitati, G. Given, C. Hicks, N. Li, B.-N. Lu, A. Rai, A. Sarkar, and J. Watkins, Projected Cooling Algorithm for Quantum Computation, *Phys. Lett. B* **807**, 135536 (2020), [arXiv:1910.07708 \[quant-ph\]](#).
- [112] K. Choi, D. Lee, J. Bonitati, Z. Qian, and J. Watkins, Rodeo Algorithm for Quantum Computing, *Phys. Rev. Lett.* **127**, 040505 (2021), [arXiv:2009.04092 \[quant-ph\]](#).
- [113] J. Hubisz, B. Sambasivam, and J. Unmuth-Yockey, Quantum algorithms for open lattice field theory, *Phys. Rev. A* **104**, 052420 (2021), [arXiv:2012.05257 \[hep-lat\]](#).
- [114] Z. Qian, J. Watkins, G. Given, J. Bonitati, K. Choi, and D. Lee, Demonstration of the Rodeo Algorithm on a Quantum Computer (2021), [arXiv:2110.07747 \[quant-ph\]](#).
- [115] A. Alexandru, P. F. Bedaque, R. Brett, and H. Lamm, Spectrum of digitized QCD: Glueballs in a S (1080) gauge theory, *Phys. Rev. D* **105**, 114508 (2022), [arXiv:2112.08482 \[hep-lat\]](#).
- [116] Y.-Y. Zou, Y. Zhou, L.-M. Chen, and P. Ye, Measuring non-Unitarity in non-Hermitian Quantum Systems (2022), [arXiv:2208.14944 \[quant-ph\]](#).
- [117] M. A. Nielsen and I. L. Chuang, *Quantum Computation and Quantum Information: 10th Anniversary Edition* (Cambridge University Press, 2010).
- [118] J. L. Park, The concept of transition in quantum mechanics, *Foundations of Physics* **1**, 23 (1970).
- [119] W. K. Wootters and W. H. Zurek, A single quantum cannot be cloned, *Nature (London)* **299**, 802 (1982).
- [120] D. Dieks, Communication by EPR devices, *Physics Letters A* **92**, 271 (1982).
- [121] V. Buzek and M. Hillery, Quantum copying: Beyond the no cloning theorem, *Phys. Rev. A* **54**, 1844 (1996), [arXiv:quant-ph/9607018](#).
- [122] H. Lamm, S. Lawrence, and Y. Yamauchi (NuQS), General Methods for Digital Quantum Simulation of Gauge Theories, *Phys. Rev. D* **100**, 034518 (2019), [arXiv:1903.08807 \[hep-lat\]](#).
- [123] M. Sohaib Alam, S. Hadfield, H. Lamm, and A. C. Y. Li, Quantum Simulation of Dihedral Gauge Theories, *arXiv e-prints*, [arXiv:2108.13305 \(2021\)](#), [arXiv:2108.13305 \[quant-ph\]](#).
- [124] I. L. Chuang and M. A. Nielsen, Prescription for experimental determination of the dynamics of a quantum black box, *J. Mod. Opt.* **44**, 2455 (1997), [arXiv:quant-ph/9610001](#).
- [125] A. R. Calderbank and P. W. Shor, Good quantum error-correcting codes exist, *Phys. Rev. A* **54**, 1098 (1996), [arXiv:quant-ph/9512032 \[quant-ph\]](#).
- [126] A. M. Steane, Error correcting codes in quantum theory, *Phys. Rev. Lett.* **77**, 793 (1996).
- [127] A. Steane, Multiple-Particle Interference and Quantum Error Correction, *Proceedings of the Royal Society of London Series A* **452**, 2551 (1996), [arXiv:quant-ph/9601029 \[quant-ph\]](#).
- [128] A. M. Steane, Simple quantum error-correcting codes, *Phys. Rev. A* **54**, 4741 (1996).
- [129] B. Eastin and E. Knill, Restrictions on transversal encoded quantum gate sets, *Physical Review Letters* **102**, 10.1103/physrevlett.102.110502 (2009).
- [130] A. Paetznick and K. M. Svore, Repeat-Until-Success: Non-deterministic decomposition of single-qubit unitaries, *arXiv e-prints*, [arXiv:1311.1074 \(2013\)](#), [arXiv:1311.1074 \[quant-ph\]](#).
- [131] I. Raychowdhury and J. R. Stryker, Loop, string, and hadron dynamics in su(2) hamiltonian lattice gauge theories, *Physical Review D* **101**, 10.1103/physrevd.101.114502 (2020).
- [132] R. Dasgupta and I. Raychowdhury, Cold-atom quantum simulator for string and hadron dynamics in non-Abelian lattice gauge theory, *Phys. Rev. A* **105**, 023322 (2022), [arXiv:2009.13969 \[hep-lat\]](#).
- [133] E. Mathew and I. Raychowdhury, Protecting local and global symmetries in simulating 1+1-D non-abelian gauge theories, *arXiv e-prints*, [arXiv:2206.07444 \(2022\)](#), [arXiv:2206.07444 \[hep-lat\]](#).
- [134] E. M. Murairi, M. J. Cervia, H. Kumar, P. F. Bedaque, and A. Alexandru, How many quantum gates do gauge theories require?, *arXiv e-prints*, [arXiv:2208.11789 \(2022\)](#), [arXiv:2208.11789 \[hep-lat\]](#).
- [135] R. Brower, S. Chandrasekharan, S. Riederer, and U.-J. Wiese, D-theory: field quantization by dimensional reduction of discrete variables, *Nuclear Physics B* **693**, 149 (2004).
- [136] B. Beard, R. Brower, S. Chandrasekharan, D. Chen, A. Tsapalis, and U.-J. Wiese, D-theory: field theory via dimensional reduction of discrete variables, *Nuclear Physics B - Proceedings Supplements* **63**, 775–789 (1998).
- [137] R. Brower, S. Chandrasekharan, and U. J. Wiese, QCD as a quantum link model, *Phys. Rev. D* **60**, 094502 (1999),

- [arXiv:hep-th/9704106 \[hep-th\]](#).
- [138] A. Ciavarella, N. Klco, and M. J. Savage, A trailhead for quantum simulation of $su(3)$ yang-mills lattice gauge theory in the local multiplet basis (2021), [arXiv:2101.10227 \[quant-ph\]](#).
- [139] E. Zohar, J. I. Cirac, and B. Reznik, Quantum simulations of gauge theories with ultracold atoms: Local gauge invariance from angular-momentum conservation, *Physical Review A* **88**, [10.1103/physreva.88.023617](#) (2013).
- [140] Y. Meurice, Examples of symmetry-preserving truncations in tensor field theory, *Phys. Rev. D* **100**, [014506](#) (2019), [arXiv:1903.01918 \[hep-lat\]](#).
- [141] Y. Meurice, Discrete aspects of continuous symmetries in the tensorial formulation of Abelian gauge theories, *Phys. Rev. D* **102**, [014506](#) (2020), [arXiv:2003.10986 \[hep-lat\]](#).
- [142] A. Bazavov, Y. Meurice, S.-W. Tsai, J. Unmuth-Yockey, and J. Zhang, Gauge-invariant implementation of the abelian-higgs model on optical lattices, *Physical Review D* **92**, [10.1103/physrevd.92.076003](#) (2015).
- [143] J. Zhang, J. Unmuth-Yockey, J. Zeiher, A. Bazavov, S.-W. Tsai, and Y. Meurice, Quantum simulation of the universal features of the polyakov loop, *Phys. Rev. Lett.* **121**, [223201](#) (2018).
- [144] J. Unmuth-Yockey, J. Zhang, A. Bazavov, Y. Meurice, and S.-W. Tsai, Universal features of the abelian polyakov loop in 1+1 dimensions, *Physical Review D* **98**, [10.1103/physrevd.98.094511](#) (2018).
- [145] Y. Ji, H. Lamm, and S. Zhu, Gluon field digitization via group space decimation for quantum computers, *Physical Review D* **102**, [10.1103/physrevd.102.114513](#) (2020).
- [146] D. González-Cuadra, T. V. Zache, J. Carrasco, B. Kraus, and P. Zoller, Hardware efficient quantum simulation of non-abelian gauge theories with qudits on Rydberg platforms, *arXiv e-prints*, [arXiv:2203.15541](#) (2022), [arXiv:2203.15541 \[quant-ph\]](#).
- [147] A. Alexandru, P. F. Bedaque, S. Harmalkar, H. Lamm, S. Lawrence, and N. C. Warrington, Gluon field digitization for quantum computers, *Physical Review D* **100**, [10.1103/physrevd.100.114501](#) (2019).
- [148] J. J. Vartiainen, M. Möttönen, and M. M. Salomaa, Efficient Decomposition of Quantum Gates, *Phys. Rev. Lett.* **92**, [177902](#) (2004), [arXiv:quant-ph/0312218 \[quant-ph\]](#).
- [149] N. P. D. Sawaya, T. Menke, T. H. Kyaw, S. Johri, A. Aspuru-Guzik, and G. G. Guerreschi, Resource-efficient digital quantum simulation of d-level systems for photonic, vibrational, and spin-s Hamiltonians, *npj Quantum Information* **6**, [49](#) (2020), [arXiv:1909.12847 \[quant-ph\]](#).

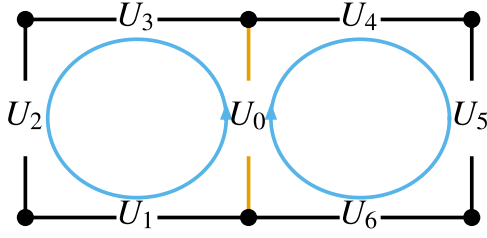


FIG. 1. Depiction of the lattice with neighboring plaquettes.

I. SMEARING ALGORITHM

1. We have a target link we want to smear, U_0 and then neighboring links $\{U_j\}$ for $j < 6D$ which form the plaquettes that connect to the target link $U_i(\vec{n})$. See Fig. 1. Two spacial dimensions is shown for example purposes.
2. We have primitive gate operations

$$\begin{aligned}
 \mathfrak{U}_x^{(a,b)}|g\rangle|h\rangle &= |gh\rangle|h\rangle \\
 \mathfrak{U}_{-1}^a|g\rangle &= |g^{-1}\rangle \\
 \mathfrak{U}_Q^{(r_0, \dots, r_{2(d-1)-1})}|g_0, \dots, g_{2(d-1)-1}\rangle|\mathbb{1}\rangle &= \\
 |g_0, \dots, g_{2(d-1)-1}\rangle|\mathcal{P}(e^{i\rho Q})\rangle
 \end{aligned} \tag{1}$$

where $|g\rangle$ and $|h\rangle$ are some quantum state corresponding to a group element, either an $SU(N)$ matrix for continuous groups or an element of a discrete group and

$$Q = \frac{1}{2}(\Omega - \Omega^\dagger) - 1/(2N)\text{Tr}(\Omega - \Omega^\dagger). \tag{2}$$

$\Omega = U_1^\dagger U_2 U_3 U_0^\dagger + U_6 U_5 U_4^\dagger U_0^\dagger + \dots$ which are the plaquettes shown in Fig. 1. The operator $\mathcal{P}(e^{i\rho Q})$ indicates to map the observable to the closest element of the group. The superscripts a and b correspond to the register the operator acts on.

3. We will proceed in 2 spacial dimensions but 3 spacial dimensions is easy to generalize to. We need to compute onto two ancilla registers the quantity $|U_6 U_5 U_4^\dagger U_0^\dagger\rangle$ and $|U_1^\dagger U_2 U_3 U_0^\dagger\rangle$
4. We can accomplish this by implementing the quantum operations

$$\begin{aligned}
 \mathfrak{U}_{p,0} &= \mathfrak{U}_{-1}^0 \mathfrak{U}_x^{(0,a_0)} \mathfrak{U}_{-1}^0 \mathfrak{U}_{-1}^4 \mathfrak{U}_x^{(4,a_0)} \mathfrak{U}_{-1}^4 \mathfrak{U}_x^{(5,a_0)} \mathfrak{U}_x^{(6,a_0)} \\
 \mathfrak{U}_{p,1} &= \mathfrak{U}_{-1}^0 \mathfrak{U}_x^{(0,a_1)} \mathfrak{U}_{-1}^0 \mathfrak{U}_x^{(3,a_0)} \mathfrak{U}_x^{(2,a_1)} \mathfrak{U}_{-1}^1 \mathfrak{U}_x^{(1,a_1)} \mathfrak{U}_{-1}^1.
 \end{aligned} \tag{3}$$

on

$$\begin{aligned}
 \mathfrak{U}_{p,0} \mathfrak{U}_{p,1} |U_0 U_1 U_2 U_3 U_4 U_5 U_6\rangle |\mathbb{1}\rangle_{a_0} |\mathbb{1}\rangle_{a_1} &= \\
 |U_0 U_1 U_2 U_3 U_4 U_5 U_6\rangle |U_6 U_5 U_4^\dagger U_0^\dagger\rangle_{a_0} |U_1^\dagger U_2 U_3 U_0^\dagger\rangle_{a_1}
 \end{aligned} \tag{4}$$

5. Then we act on the ancilla registers with $\mathfrak{U}_Q^{(r_0, \dots, r_{2(d-1)-1})}$ as

$$\begin{aligned}
 \mathfrak{U}_Q^{(a_0, a_1)} |U_6 U_5 U_4^\dagger U_0^\dagger\rangle_{a_0} |U_1^\dagger U_2 U_3 U_0^\dagger\rangle_{a_1} |\mathbb{1}\rangle &= \\
 |U_6 U_5 U_4^\dagger U_0^\dagger\rangle_{a_0} |U_1^\dagger U_2 U_3 U_0^\dagger\rangle_{a_1} |\mathcal{P}(e^{i\rho Q})\rangle
 \end{aligned} \tag{5}$$

6. We now uncompute the ancilla registers $|\rangle_{a_0}$ and $|\rangle_{a_1}$ using $\mathfrak{U}_{p,0}^\dagger$ and $\mathfrak{U}_{p,1}^\dagger$.
7. this uncomputation allows us to reclaim used qubits and avoid an extremely large resource bloat.
8. repeat steps 4 - 7 for every link.
9. multiply each ancilla register onto its corresponding original link via \mathfrak{U}_x .
10. we are left with an entire lattice worth of qubits that we can't uncompute.